

JAERI-M
87-035

LEACHING BEHAVIOR OF SIMULATED HIGH-LEVEL
WASTE GLASS

March 1987

Hiroshi KAMIZONO

JAERI Mレポートは、日本原子力研究所が不定期に公刊している研究報告書です。

入手の間合わせは、日本原子力研究所技術情報部情報資料課（〒319 11 茨城県那珂郡東海村）あて、お申しこしてください。なお、このほかに財団法人原子力弘済会資料センター（〒319 11 茨城県那珂郡東海村日本原子力研究所内）で複写による実費領布をおこなっております。

JAERI M reports are issued irregularly.

Inquiries about availability of the reports should be addressed to *Information Division Department of Technical Information, Japan Atomic Energy Research Institute, Tokaimura, Naka gun, Ibaraki ken 319 11, Japan.*

© Japan Atomic Energy Research Institute, 1987

編集兼発行 日本原子力研究所
印 刷 日青工業株式会社

Leaching Behavior of Simulated High-Level Waste Glass

Hiroshi KAMIZONO

Department of Environmental Safety Research,

Tokai Research Establishment,

Japan Atomic Energy Research Institute,

Tokai-mura, Naka-gun, Ibaraki-ken

(Received February 5, 1987)

The author's work in the study on the leaching behavior of simulated high-level waste (HLW) glass were summarized. The subjects described are (1) leach rates at high temperatures, (2) effects of cracks on leach rates, (3) effects of flow rate on leach rates, and (4) an in-situ burial test in natural groundwater. In the following section, the leach rates obtained by various experiments were summarized and discussed.

Keywords: High-Level Radioactive Waste, Borosilicate Glass, Leach Rates, High Temperatures, Thermal Cracks, Flow Rates, In-situ burial tests, Geologic Disposal

模擬ガラス固化体の浸出挙動

日本原子力研究所東海研究所環境安全研究部

上 蘭 裕 史

(1987年 2月 5日 受理)

模擬高レベル廃棄物固体の浸出挙動に関する著者の研究について、(1)高温での浸出挙動、(2)浸出率に対する亀裂の効果、(3)浸出率に対する流速の効果、(4)天然地下水中での原位置試験、の4項目について整理した。

さらに各種の条件下での浸出試験で得られた浸出率を相互比較し検討した。

Contents

1. Introduction	1
2. Leach Rates at High Temperatures	1
3. Effects of Cracks on Leach Rates	2
4. Effects of Flow Rate on Leaching Behavior	4
5. In-situ Burial Test in Natural Groundwater	5
6. Leach Rates under Various Conditions	6
7. Remarks for Further Research	8
Acknowledgement	9
References	10

目 次

1. 序 論	1
2. 高温での浸出率	1
3. 亀裂の効果	2
4. 流速の効果	4
5. 原位置浸出試験	5
6. 各種条件下での浸出率	6
7. 結 語	8
謝 辞	9
文 献	10

1. Introduction

High-level liquid waste stemming from the spent fuel reprocessing plant contains hazardous fission products and actinides, and should be isolated from the biosphere. One isolation method is solidification of the liquid as borosilicate glass and subsequent storage and disposal. Disposal sites may be constructed in geologic formations more than several hundred meters below the surface. Therefore, the contact of groundwater with high-level waste (HLW) glass is one of the major concerns, and much attention has been paid to the study of the leaching phenomena of HLW glass.^(1,2)

The objective of the present report is to summarize the author's work⁽³⁻¹⁰⁾ in the study on the leaching behavior of HLW glass. Broad reviews relating to the HLW glass leaching are beyond the scope of the present report. The subjects described here are (1) leach rates at high temperatures, (2) effects of cracks on leach rates, (3) effects of flow rate on leach rates, and (4) one example of an in-situ burial test in natural groundwater. Each of these is described as an isolated subject, however in the following section leach rates under various conditions are summarized in one figure and relative importance of various factors is noted.

2. Leach Rates at High Temperatures

Leach tests at high temperatures will provide useful information about the leaching behavior of HLW glass in accidents such as water penetration in geologic disposal sites. Also, temperature is a factor which may accelerate leaching behavior, and therefore may be useful to

predict long-term leach rates at relatively lower temperatures.

The author studied the leachability of simulated HLW glass at 100-280°C (64 atm) by using a Soxhlet-type leaching device (HIPSOL).⁽³⁾ The glass leached in the temperature range was observed by an optical microscope, a scanning electron microscope with wave dispersive X-ray analysis, and a X-ray diffractometer.

Figure 1 shows that the surface of the glass changes with increasing temperature.⁽³⁾ Below 150°C, narrow cracks appear on the surface, indicating the formation of a thin altered layer on the surface. Above 220°C, in contrast, the surface changes markedly. The production of many precipitates rich in Ca and a crystal phase (analcite, $\text{NaAl}(\text{SiO}_3)_2 \cdot 2\text{H}_2\text{O}$) occur. In addition, relatively large cracks appear at 280°C (Fig.1(e)) and fragments of the glass appear in the leachate (an arrow in Fig.1(f)). The Arrhenius plots for various elements showed that the activation energy rose sharply for more than 220°C.

The results described above imply that the leaching behavior of simulated HLW glass is changed at a temperature between 150°C and 220°C in a straight line on the Arrhenius plots. Westsik et al.^(11,12) obtained the results on the leach rates for B, Mo, Na and Si, in a straight line from 50°C up to 150°C on the Arrhenius plots, however, they did not try the microscopic observation at the leached glass.

3. Effects of cracks on leach rates

HLW glass in a canister will have some cracks produced through the

cooling process after vitrification, or by mechanical impact during transportation.

The author conducted static leach tests at 100°C for 1 h in order to examine the influences of thermally induced cracks on leach rates. Figure 2 shows the relationship of the fractional release of Na and Cs from the quenched specimens with the quenching temperature. The fractional release is almost constant in the range of temperature difference up to 500°C, but greatly increases at a temperature difference of 600°C. The initiation of thermal cracks began at a temperature difference of 74°C, but the specimen tended to maintain its monolithic form up to a temperature difference of 500°C. However at a temperature difference of 600°C, the glass fragmented. The surface area of the fragments after quenching at the temperature difference of 600°C was calculated to be about 8.6 times that of the original specimen, and the leach rate after quenching at the temperature difference of 600°C is about 9.2 times higher than that after the temperature difference of 500°C. Therefore, the increase in leach rates is considered to result mainly from the increase of the surface area.

The results indicate that leaching from the surface cracks is nearly independent of the density of cracks in short period leaching, but dependent on the separation of the fracture surfaces. Perez et al.⁽¹³⁾ have examined the effects of artificial cracks on leach rates and also showed that leaching from crack surfaces with nominally zero crack widths does not occur.

4. Effects of Flow Rate on Leaching Behavior

One important factor which affect HLW glass leaching in the geologic disposal sites will be the flow rate of groundwater, since geologic repository system may be open to the inflow and outflow of groundwater.

The author has confirmed that, as shown in Fig.3, leach rates for Si in both synthesized groundwater and deionized water are increased nearly proportional to flow rates of leachant with increasing flow rates in the range of 0.001 to 0.1 ml/min^(7,10). These results can be interpreted to mean that, as flow rates increase, the concentration of Si decreases in water adjacent to the glass, therefore the inhibition by the buildup of solution products becomes less effective.

Hench et al.⁽²⁾ have described that the steady-state leach rate (R_{SS} (g/cm²day)) can be defined in terms of the flow rate (f (ml/day)), saturation concentration (C_s (g/ml)) and surface area of the glass (S (cm²)), thus,

$$R_{SS} = KC_s f / (SK + f) \quad (1)$$

where K is a leach rate constant (cm/day). Equation (1) indicates that the leach rate is expected to be dependent on the flow rate. At low flow rates, R_{SS} is close to fC_s/S , and R_{SS} should be proportional to the flow rate. Our experimental results agree with Hench et al.'s analysis.

It should be mentioned that in our experiments the increase of a solution pH may cause the increase of leach rates at low flow rates. This can be seen in Fig.3 in the case of deionized water. Although

leach rates increase by a factor of less than three by this pH effect (Fig.3), this calls our attention to the increase of leach rates at low flow rates.

5. In-situ Burial Test in Natural Groundwater

The author has first hand knowledge of one example of an in-situ burial leach test for up to one year and seven months.^(6,8,9) One characteristic of the natural groundwater was the fact that it contained a considerable amount of HCO_3^- and SO_4^{-2} anions.

Figure 4 shows a scanning electron micrograph of the surface of the specimen leached in the natural groundwater at 14°C for one year and seven months. It is assumed that the leaching behavior of the glass is divided into two categories; one is leaching from the flat surface and the other is that from the grooves, and only the extent of leaching from the flat surface can be measured by a scanning electron microscope with energy dispersive X-ray analysis (SEM-EDX)⁽⁶⁾. We define the C/C_0 -value as the ratio of the concentration of Na on the flat surface of a leached specimen (C) to the initial concentration of Na before leaching (C_0). The values of C and C_0 are measured by SEM-EDX with the electron beam rapidly scanning over the flat surface of the specimen for an area of about $20 \times 20 \mu\text{m}$ for 200 sec. A constant accelerating voltage of 20 keV and a constant probe current of 10^{-10} A were used. The glass before leaching was used as a standard for Na of 8.38 wt%, and the accuracy of the C/C_0 -value was confirmed by repeating the measurement six times. Any tendency for the amount of Na to decrease during the scanning of the electron beam was not

observed.⁽¹⁴⁾

Figure 5 shows the relationship between the C/C_0 -value of Na and the normalized elemental mass losses for Na (NL_{Na} (g/cm^2)). In the case of deionized water, a single line is observed between the C/C_0 -values and NL_{Na} either at 20°C or 100°C. However, the line for the case of synthesized groundwater is placed on the right hand side, and this can be attributed to the occurrence of the grooves, thus the leaching of Na from the grooves can increase the overall leach rate.

It is possible to estimate the order of NL_{Na} by measuring the extent of leaching of the flat surface by SEM-EDX and by measuring the size and the number of the grooves by a microscope, and by this method the leach rate of 8×10^{-7} g/cm^2 day in the natural groundwater was obtained.⁽⁹⁾ Although leach rates in the natural environment have not been shown, extensive in-situ burial leach tests have been carried out in the Stripa mine in Sweden⁽¹⁵⁻¹⁷⁾.

6. Leach Rates under Various Conditions

Leach rates for sodium are generally equal to or higher than those of the other elements, and therefore can be used as conservative values for assessing the safety of HLW glass.

The leach rates for sodium obtained in the author's work are summarized in Fig.6. The y-axis of this figure represents leach rates with the unit of g/cm^2 day. This unit means that there are two tacit assumptions; i.e., (1) the surface area of the glass does not change markedly during leach tests, (2) the time-dependence of normalized elemental mass loss (NL) can be expressed as,

$$NL = kt \quad (2)$$

where k is a constant which includes the Arrhenius-type temperature-dependence, and t is time in days. Thus, leach rates for an element in the glass ($R(\text{g}/\text{cm}^2\text{day})$) is,

$$R = dNL/dt = k \text{ (constant)} \quad (3)$$

The leach rates in Fig.6 increase from an order of 10^{-7} $\text{g}/\text{cm}^2\text{day}$ at room temperature to an order of 10^{-1} $\text{g}/\text{cm}^2\text{day}$ at about 280°C , however they seem to fall in a narrow range between curved lines (1) and (2). These lines tend to decline for temperatures of more than 100°C , and this tendency has been also observed by Westsik et al.^(11,12) for the temperatures of more than 150°C . Small particles were used for our experiments (plots of \bullet), and this can be a cause for the leachable surface to decrease to a certain extent during leaching, thereby resulting in the decrease of apparent leach rates at high temperatures. Another possibility is that the activation energy of the glass used for the experiments of more than 100°C is lower than that of the glass for temperatures of less than 100°C .

Plots of \square and \square show that the leach rate in synthesized groundwater is almost the same as that in deionized water, which is also very close to the leach rate in natural groundwater (plot of \square). Three plots of \blacktriangle 1, \blacktriangle 2 and \blacktriangle 3 show the effects of flow rates in the range from zero to 0.1 ml/min. on leach rates within one order of magnitude. Three plots at 100°C of \bullet , \blacksquare and \circ show that leach rates of three different kinds of glass (38.3wt% SiO_2 +14.0wt%waste, 48.5wt% SiO_2 +11.7wt%waste and 52.1wt% SiO_2 +14.0wt%waste, respectively) are within one order of

magnitude. Thus the effects of water composition, flow rates of water and glass composition on leach rates may not be very large in comparison with those of temperature.

Additionally, since line 3 seems to be straight in Fig.6, the apparent activation energy can be calculated to be 77 kJ/mol (18 kcal/mol) for temperatures of less than 100°C. This value is within the range of 40 to 80 kJ/mol obtained for various kinds of borosilicate glass⁽¹⁸⁾. The activation energy of 18 kcal/mol^{0K} calculated above is large enough to imply that the rate limiting step for sodium is not the diffusion through an altered surface layer. Instead, it is speculated that a possible mechanism is the congruent dissolution of the glass network structure on the boundary between an altered surface layer and the bulk of the glass. However, this is not true for other elements such as Mg, Mn, Fe, Ni, Zr, Ba and REE, since Murakami et al.⁽¹⁹⁾ have noted that the elements tend to remain in the altered surface layers.

7. Remarks for Further Research

Since the period for HLW glass to be in contact with groundwater is expected to be very long, leach experiments during such a long period are absolutely impossible in laboratories, therefore it is quite important to carry out accelerated leach tests.

Although concepts for accelerated leach tests have not been fully developed, there are at least two factors which could accelerate the leaching behaviors of HLW glass. One is the temperature (the author's work^(3,8), and Westsik et al.^(11,12)) and the other is the ratio of

the surface area of the specimen to the solution volume (S/V-ratio) (Pederson et al.⁽²⁰⁾, and Stahl et al.⁽²¹⁾). It is considered that there are shortcomings in either method; in the former method, mechanisms of leaching may be changed at different temperatures, or in the latter method, the static conditions with a high S/V-ratio generally needs fine grained particles which will produce the complexity coming from direct contacts between the particles. Thus, the above two methods may supplement each other and it is speculated that better description of the accelerated results can be obtained by the combination of those methods.

Acknowledgement

The author thanks Dr. H. Nakamura and Mr. T. Banba for their comments on the manuscript.

References

- (1) Compiled by J.E. Mendel, "Final Report of the Defense High-Level Waste Leaching Mechanisms Program," PNL-5157, Pacific Northwest Laboratory, Richland, Washington (1984).
- (2) L.L. Hench, D.E. Clark and A.B. Harker, "Review, Nuclear Waste Solids," J. Mater. Sci., 21, 1457-1478 (1986).
- (3) H. Kamizono, T. Banba, M. Senoo, S. Tashiro, K. Araki and H. Amano, "Leachability of a Simulated High-Level Waste Glass Product at High Temperatures," JAERI-M 9387 (1981).
- (4) H. Kamizono and M. Senoo, "Thermal Shock Resistance of a Simulated High-Level Waste Glass," Nucl. Chem. Waste Manage., 4, 329-333 (1983).
- (5) H. Kamizono and T. Banba, "A Relationship between Leach Rate of Nuclear Waste Glass and Residual Amount of Sodium on the Glass Surface," JAERI-M 84-220 (1984).
- (6) H. Kamizono, "Leaching Behavior of Simulated High-Level Waste Glass in Groundwater," J. Nucl. Mater., 127, 242-246 (1985).
- (7) I. Shimizu and H. Kamizono, "Leaching Behavior of Simulated High-Level Waste Glass in Flowing Water," JAERI-M 86-070 (1986).
- (8) H. Kamizono and T. Banba, "Comparison of Nuclear Waste Glass Leached in Natural Groundwater at 14°C with That in Synthesized Groundwater at 70°C," J. Nucl. Sci. Technol., 23, 755-758 (1986).
- (9) H. Kamizono and H. Nakamura, "Simulated High-Level Nuclear Waste Glass Leached in Groundwater," submitted to J. Non-Crystal. Solids.
- (10) H. Kamizono, I. Shimizu and T. Banba, "Dynamic and Static Leach

Tests of Simulated High-Level Waste Glass in Synthesized Groundwater and Deionized Water," submitted to J. Nucl. Sci. Technol.

- (11) J.H. Westsik, Jr. and R.D. Peters, "Time and Temperature Dependence of the Leaching of a Simulated High-Level Waste Glass," PNL-SA-9054 (1980).
- (12) J.H. Westsik, Jr., J.W. Shade and G.L. McVay, "Temperature Dependence for Hydrothermal Reactions of Waste Glasses and Ceramics," in Scientific Basis for Nuclear Waste Management Vol.2, Edited by C.J.M. Northrap, Jr., Plenum Press, New York, pp.239-248 (1980).
- (13) J.M. Perez, Jr. and J.H. Westsik, Jr., "Effects of Cracks on Glass Leaching," Nucl. Chem. Waste Manage., 2, 165-168 (1981).
- (14) P.J. Goodhew and J.E.C. Gulley, "The Determination of Alkali Metals in Glasses by Electron Probe Microanalysis," Glass Technol., 15 123-126 (1974).
- (15) L.L. Hench, A. Lodding and L. Werme, "Nuclear Waste Glass Interfaces after One Year Burial in Stripa, Part 1: Glass/Glass," J. Nucl. Mater., 125, 273-279 (1984).
- (16) A. Lodding, L.L. Hench and L. Werme, "Nuclear Waste Glass Interfaces after One Year Burial in Stripa, Part 2: Glass/Bentonite," J. Nucl. Mater., 125, 280-286 (1984).
- (17) L.L. Hench, L. Werme and A. Lodding, "Nuclear Waste Glass Interfaces after One Year Burial in Stripa, Part 3: Glass/Granite," J. Nucl. Mater., 126, 226-233 (1984).
- (18) International Atomic Energy Agency, "Chemical Durability and

Related Properties of Solidified High-Level Waste Forms," Draft of Technical Report Series (November, 1983).

- (19) T. Murakami and T. Banba, "Leaching Behavior of a Glass Waste Form- Part I: The Characteristics of Surface Layers," Nucl. Technol., 67, 419-428 (1984).
- (20) L.R. Pederson, C.Q. Buckwalter and G.L. McVay, "The Effects of Surface Area to Solution Volume on Waste Glass Leaching," Nucl. Technol., 62, 151-158 (1983).
- (21) Compiled by D. Stahl and N.E. Miller, "Long-Term Performance of Materials Used for High-Level Waste Packaging," NUREG/CR-4379 Vol.2 (1985).

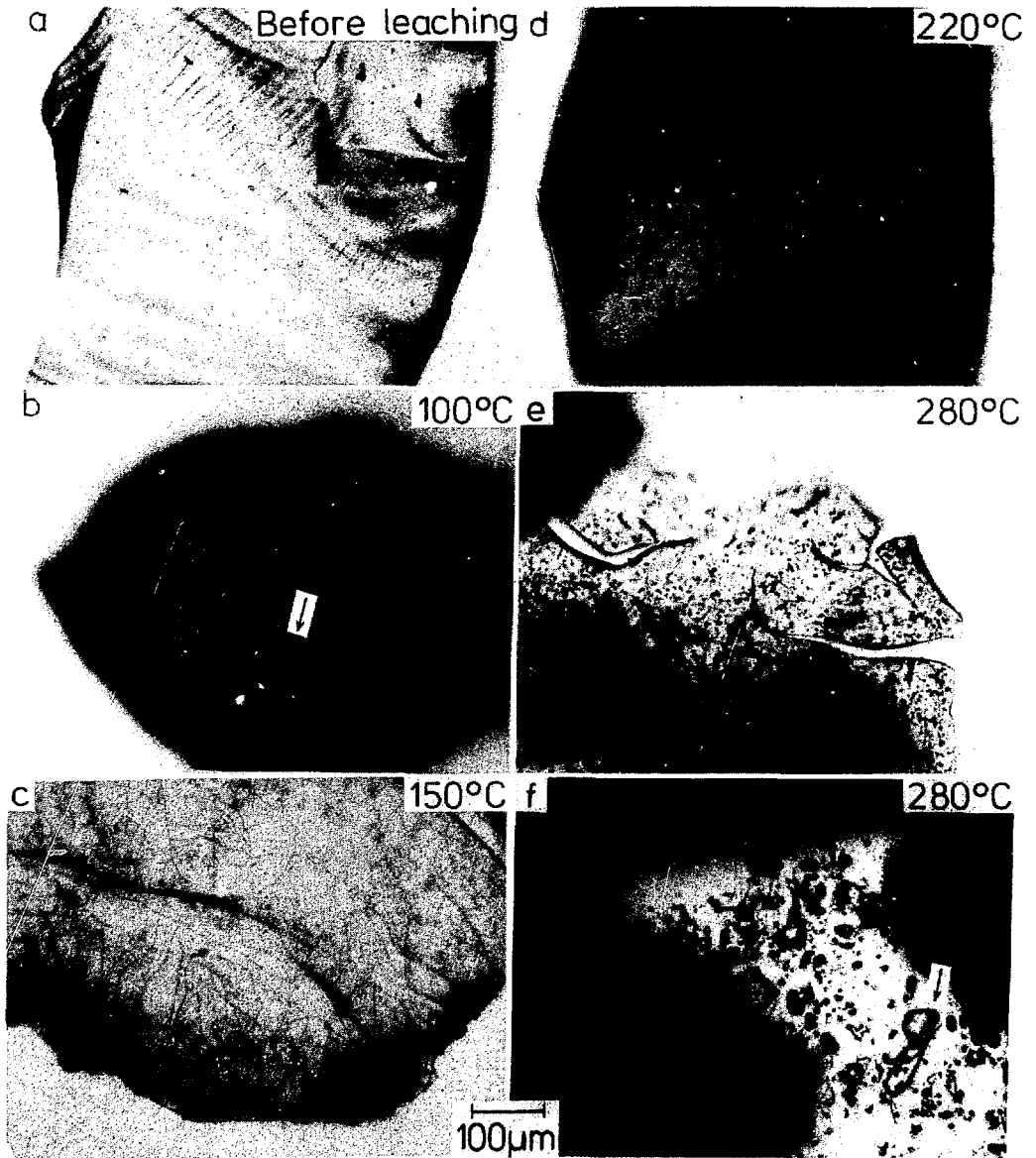


Fig.1 Optical microphotographs of the specimens before and after leach tests. Before leaching (a), leached at 100°C for 8 h (b), at 150°C for 8 h (c), at 220°C for 8 h (d), at 280°C for 8 h (e), and near the glass leached at 280°C (f).

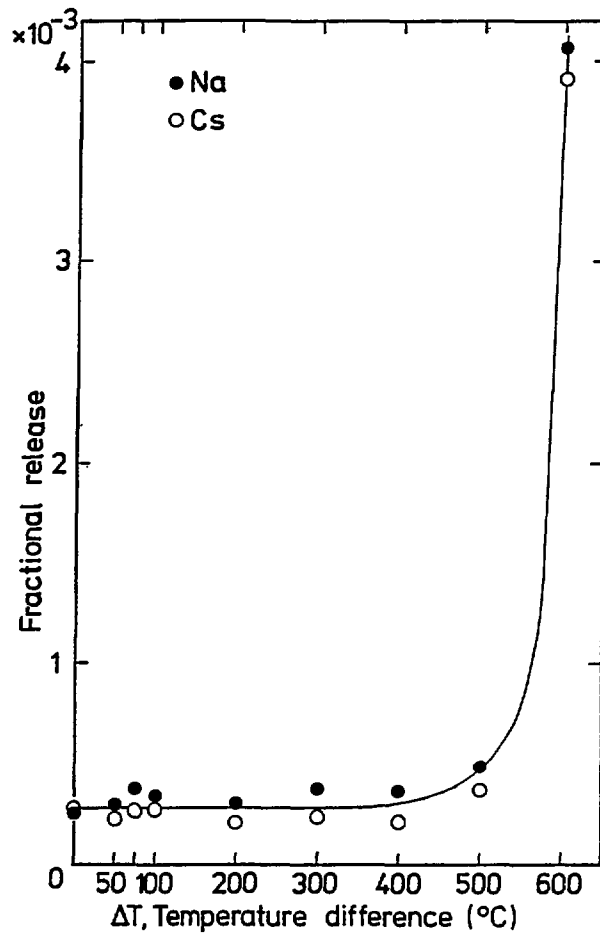


Fig.2 Relationship between the fractional release of Na and Cs and the temperature difference.

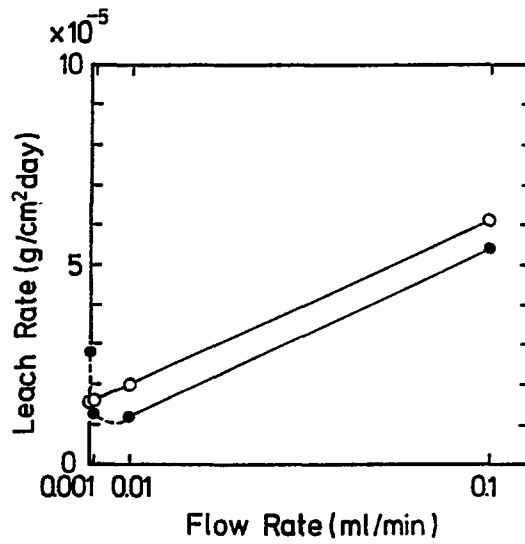


Fig.3 Relationship between the leach rates of Si and the flow rates at 70°C.

- ; in deionized water.
- ; in synthesized groundwater.



Fig.4 Scanning electron microphotograph of the surface of the specimen leached in natural groundwater at 14°C for one year and seven months.

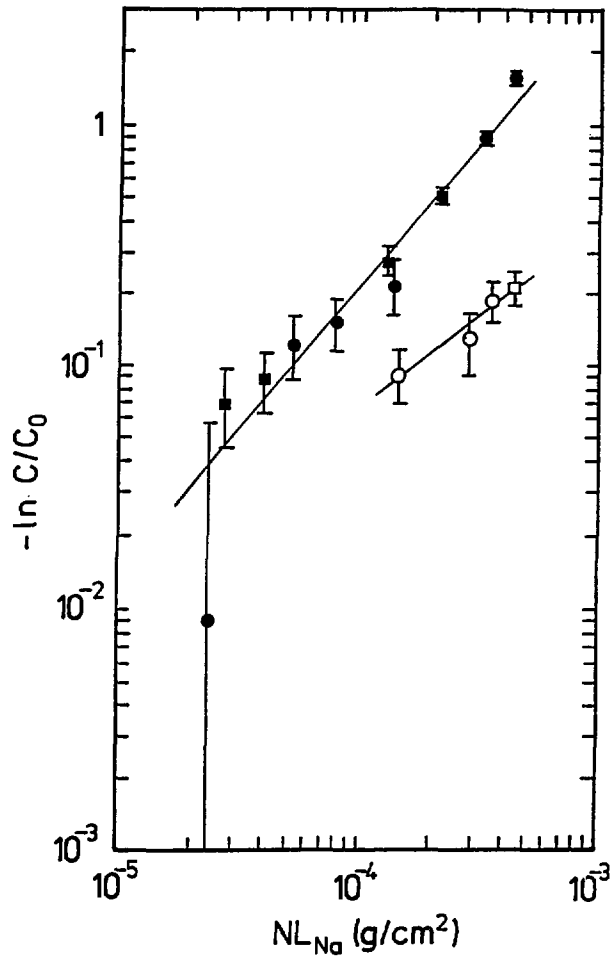


Fig.5 Relationship between the C/C_0 -values of Na and normalized elemental mass losses for Na (NL_{Na}).

- ; in deionized water at 100°C.
- ; in deionized water at 20°C.
- ; in synthesized groundwater at 20°C.
- ; in synthesized groundwater at 70°C.

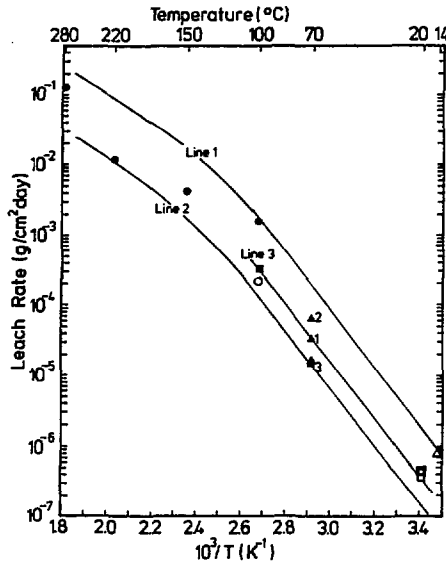


Fig.6 Relationship between leach rates of Na in $\text{g/cm}^2\text{day}$ and reciprocal absolute temperature.

- ; deionized water, 100–280°C, dynamic (HIPSOL), J-10 glass, JW-B waste.(3)
- ; deionized water, 100°C, static, typical simulated HLW glass (T-SHLW-G), JW-D waste.(5)
- ; deionized water, 100°C, static, borosilicate glass, JW-C waste.(4)
- ▲ ; synthesized groundwater, 70°C, static, T-SHLW-G, JW-D waste.(7)
- ▲1; deionized water, 70°C, static, T-SHLW-G, JW-D waste.(7)
- ▲2; deionized water, 70°C, dynamic (0.1 ml/min.), T-SHLW-G, JW-D waste.(7)
- ▲3; deionized water, 70°C, dynamic (0.001 ml/min.), T-SHLW-G, JW-D waste.(7)
- ▣ ; synthesized groundwater, 20°C, static, T-SHLW-G, JW-D waste.(6)
- ; deionized water, 20°C, static, T-SHLW-G, JW-D waste.(6)
- △ ; natural groundwater, 14°C, dynamic (0.007–0.14 ml/min.) T-SHLW-G, JW-D waste.(9)

国際単位系 (SI) と換算表

表1 SI基本単位および補助単位

属	名称	記号
長さ	メートル	m
質量	キログラム	kg
時間	秒	s
電流	アンペア	A
熱力学温度	ケルビン	K
物質質量	モル	mol
光度	カンデラ	cd
平面角	ラジアン	rad
立体角	ステラジアン	sr

表3 固有の名称をもつSI組立単位

量	名称	記号	他のSI単位による表現
周波数	ヘルツ	Hz	s ⁻¹
力	ニュートン	N	m·kg/s ²
圧力、応力	パスカル	Pa	N/m ²
エネルギー、仕事、熱量	ジュール	J	N·m
仕事率、放射束	ワット	W	J/s
電気量、電荷	クーロン	C	A·s
電位、電圧、起電力	ボルト	V	W/A
静電容量	ファラド	F	C/V
電気抵抗	オーム	Ω	V/A
コンダクタンス	シーメンス	S	A/V
磁束	ウェーバ	Wb	V·s
磁束密度	テスラ	T	Wb/m ²
インダクタンス	ヘンリー	H	Wb/A
セルシウス温度	セルシウス度	°C	
光量	セルシウス度	lm	cd·sr
照射度	ルクス	lx	lm/m ²
放射能	ベクレル	Bq	s ⁻¹
吸収線量	グレイ	Gy	J/kg
線量当量	シーベルト	Sv	J/kg

表2 SIと併用される単位

名称	記号
分、時、日	min, h, d
度、分、秒	°, ', "
リットル	l, L
トン	t
電子ボルト	eV
原子質量単位	u

1 eV = 1.60218 × 10⁻¹⁹ J

1 u = 1.66054 × 10⁻²⁷ kg

表4 SIと共に暫定的に維持される単位

名称	記号
オンクストローム	Å
バール	bar
ガロン	Gal
キュリー	Ci
レントゲン	R
ラデ	rad
レム	rem

1 Å = 0.1 nm = 10⁻¹⁰ m

1 bar = 100 fm² = 10⁻⁷ m²

1 bar = 0.1 MPa = 10⁵ Pa

1 Gal = 1 cm/s² = 10⁻² m/s²

1 Ci = 3.7 × 10¹⁰ Bq

1 R = 2.58 × 10⁻⁴ C/kg

1 rad = 1 cGy = 10⁻² Gy

1 rem = 1 cSv = 10⁻² Sv

表5 SI接頭語

指数	接頭語	記号
10 ¹⁸	エクサ	E
10 ¹⁵	ペタ	P
10 ¹²	テラ	T
10 ⁹	ギガ	G
10 ⁶	メガ	M
10 ³	キロ	k
10 ²	ヘクト	h
10 ¹	デカ	da
10 ⁻¹	デシ	d
10 ⁻²	センチ	c
10 ⁻³	ミリ	m
10 ⁻⁶	マイクロ	μ
10 ⁻⁹	ナノ	n
10 ⁻¹²	ピコ	p
10 ⁻¹⁵	フェムト	f
10 ⁻¹⁸	アト	a

(注)

- 表1 5は「国際単位系」第5版、国際度量衡局 1985年刊行による。ただし、1 eV および 1 uの値はCODATAの1986年推奨値によった。
- 表4には海里、ノット、アール、ヘクタールも含まれているが日常の単位なのでここでは省略した。
- barは、JISでは流体の圧力を表す場合に限り表2のカテゴリに分類されている。
- EC開僚理事会指令では bar, barn および「血圧の単位」mmHgを表2のカテゴリに入れていない。

換算表

力	N (=10 ⁵ dyn)	kgf	lbf
1	1	0.101972	0.224809
9.80665	1	1	2.20462
4.44822	1	0.453592	1

粘度 1 Pa·s (N·s/m²) = 10 P (ポアズ) (g/(cm·s))

動粘度 1 m²/s = 10⁶ St (ストークス) (cm²/s)

圧	MPa (=10 bar)	kgf/cm ²	atm	mmHg (Torr)	lbf/in ² (psi)
1	1	10.1972	9.86923	7.50062 × 10 ¹	145.038
力	0.0980665	1	0.967841	735.559	14.2233
	0.101325	1.03323	1	760	14.6959
	1.33322 × 10 ⁻⁴	1.35951 × 10 ⁻¹	1.31579 × 10 ⁻¹	1	1.93368 × 10 ⁻²
	6.89476 × 10 ⁻¹	7.03070 × 10 ⁻²	6.80460 × 10 ⁻²	51.7149	1

エネルギー	J (=10 ⁷ erg)	kgf·m	kW·h	cal (計量法)	Btu	ft·lbf	eV
1	1	0.101972	2.77778 × 10 ⁻⁷	0.238889	9.47813 × 10 ⁻⁴	0.737562	6.24150 × 10 ¹⁸
9.80665	1	1	2.72407 × 10 ⁻⁶	2.34270	9.29487 × 10 ⁻⁴	7.23301	6.12082 × 10 ¹⁸
3.6 × 10 ⁶	3.67098 × 10 ⁵	1	1	8.59999 × 10 ⁵	3412.13	2.65522 × 10 ⁶	2.24694 × 10 ¹⁹
4.18605	0.426858	1.16279 × 10 ⁻⁶	1	1	3.96759 × 10 ⁻¹	3.08747	2.61272 × 10 ¹⁸
1055.06	107.586	2.93072 × 10 ⁻⁴	1	252.042	1	778.172	6.58515 × 10 ¹¹
1.35582	0.138255	3.76616 × 10 ⁻²	1	0.323890	1.28506 × 10 ⁻¹	1	8.46233 × 10 ¹⁸
1.60218 × 10 ⁻¹⁹	1.63377 × 10 ⁻²⁰	4.45050 × 10 ⁻²⁶	1	3.82743 × 10 ⁻²⁶	1.51857 × 10 ⁻²²	1.18171 × 10 ⁻¹⁹	1

1 cal = 4.18605 J (計量法)

= 4.184 J (熱化学)

= 4.1855 J (15 °C)

= 4.1868 J (国際蒸気表)

仕事率 1 PS (仏馬力)

= 75 kgf·m/s

= 735.499 W

放射能	Bq	Ci
1	1	2.70270 × 10 ⁻¹¹
3.7 × 10 ¹⁰	1	1

吸収線量	Gy	rad
1	1	100
0.01	1	1

照射線量	C/kg	R
1	1	3876
2.58 × 10 ⁻⁴	1	1

線量当量	Sv	rem
1	1	100
0.01	1	1